Journal of Applied Mechanics and Technical Physics, Vol. 39, No. 2, 1998

THE SHOCK-WAVE STRUCTURE IN A TWO-VELOCITY MIXTURE OF COMPRESSIBLE MEDIA WITH DIFFERENT PRESSURES

A. A. Zhilin and A. V. Fedorov

UDC 532.529

The problem of the shock-wave structure in a mixture of two compressible media with different velocities and pressures of components is considered. The problem is reduced to solving a boundary-value problem for two ordinary differential equations that describe the velocity relaxation and pressure equalization of the components. Using methods of the qualitative theory of dynamic systems on a plane, the existence and uniqueness of four types of waves are shown: (a) *fully dispersed waves;* (b) *frozen-dispersed waves;* (c) *dispersed-frozen waves;* (d) *frozen waves of two-front configuration. A chart of solutions of the corresponding flow types is constructed in the plane of the following parameters: the initial velocity of the mixture and the initial volume concentration of one of the components. The numerical calculations conducted illustrate the obtained analytical structures of the shock wave. It is shown that the results obtained using the suggested mathematical model are in agreement with experimental data on the dependence of the velocity of the dispersed shock wave on the equilibrium pressure behind the shock-wave front for a mixture of silica sand and water.*

In [1–3], the structure of a shock wave (SW) in a mixture of two solids is described in the hydrodynamic approximation of one- and two-velocity flow with different pressures of the components and two-velocity flow with equal pressures of the components. In [4], the stability of propagation of various SW types found in [1–3] is shown numerically and the problem of SW reflection from a rigid wall is solved. The SW structure in a one-velocity and one-temperature flow of a mixture with different pressures is studied in [5].

In the present paper, we consider the problem of description of an SW in a mixture of two compressible media in the case of variable (in contrast to [2]) concentrations of the components and their different velocities and pressures.

1. Governing Equations and Formulation of the Problem. The equations that describe the flow of a mixture of two compressible media with different pressures and velocities of the phases have the following form in a coordinate system propagating together with the SW:

$$U_1\dot{\rho}_1 + \rho_1\dot{U}_1 = 0, \quad U_2\dot{\rho}_2 + \rho_2\dot{U}_2 = 0, \quad C_1\dot{U}_1 + C_2\dot{U}_2 + \dot{P} = 0,$$
$$C_2\dot{U}_2 + m_2\dot{P}_2 + (P_2 - P_1)\dot{m}_2 + F_S = 0, \quad \dot{m}_2 = R. \tag{1.1}$$

Here and below, m_i is the volume concentration of the ith phase ($m_1 + m_2 = 1$), $P = P_1m_1 + P_2m_2$ is the pressure in the mixture, $P_i = a_i^2(\rho_{ii} - \rho_{ii,0})$ is the pressure of the ith phase, $\rho = \rho_1 + \rho_2$ is the density of the mixture, $\rho_i = \rho_{ii}m_i$ is the mean density of the ith phase, ρ_{ii} is the true density of the ith phase, $\rho_{ii,0}$ is the true initial density of the ith phase, $\xi_i = \rho_i/\rho$, $C_0 = \rho_0U_0 = C_1 + C_2$, $C_i = \rho_{i0}U_0$, $C_3 = (C_1 + C_2)U_0$, $C = 1 - a^2\bar{\rho}$, $a = a_2/a_1$, $\bar{\rho} = \rho_{22,0}/\rho_{11,0}$, U_i is the relative velocity of the ith phase, a_i is the speed of sound in the ith phase, $R = m_1m_2(P_2 - P_1)/(\mu_2U_2)$ is the function that describes the process of pressure equalization in the phases [6], $F_S = m_1\rho_2(U_2 - U_1)/\tau_S$ is the Stokes force that takes into account the interaction between

Institute of Theoretical and Applied Mechanics, Siberian Division, Russian Academy of Sciences, Novosibirsk 630090. Translated from Prikladnaya Mekhanika i Tekhnicheskaya Fizika, Vol. 39, No. 2, pp. 10–19, March–April, 1998. Original article submitted June 6, 1996; revision submitted July 19, 1996.

 0021-8944/98/3902-0166 $20.00

the phases due to viscosity, $\tau_S = 2\rho_{22}r^2/(9\mu_1)$ is the time of Stokes relaxation of velocities, r is the radius of a solid particle, μ_i is the dynamic viscosity of the ith phase, and $\tau_{m_2} = 2\mu_2/(a_1^2\rho_{11,0})$.

Since the mixture is in a state of dynamic and thermodynamic equilibrium upstream of the shock-wave front and far downstream of it, we should impose for (1.1) the conditions of steadiness at $\pm\infty$ for the vector of the solution $\Phi(\rho_1, \rho_2, U_1, U_2, P, m_2)$:

$$\Phi \to \Phi_0, \quad \Phi_{\text{fin}}, \quad \dot{\Phi} \to 0 \qquad \text{for } \zeta \to \pm\infty. \tag{1.2}$$

Thus, the physical problem of propagation of a steady shock wave in a mixture of two materials reduces to the solution of the boundary-value problem (1.1) and (1.2).

System (1.1) reduces to the usual Cauchy problem for two ordinary differential equations:

$$\frac{dU_1}{d\zeta} = \frac{U_1}{\rho_1}\frac{F_S - \rho_1 R/m_1}{U_1^2 - 1}, \qquad \frac{dU_2}{d\zeta} = -\frac{U_2}{\rho_2}\frac{F_S + R[P_2 - P_1 - a^2\rho_2/m_2]}{U_2^2 - a^2}. \tag{1.3}$$

The function m_1 is found from the law of conservation of momentum for the mixture

$$C_1U_1 + C_2U_2 + P(\rho_1, \rho_2, m_1) = C_3$$

and equations $\rho_i = C_i/U_i$ in the form

$$m_1 = \frac{C_1U_2(U_1^2 + 1) + C_2U_1(U_2^2 + a^2) - U_1U_2(C_3 + a^2\bar{\rho})}{CU_1U_2}.$$

2. Possible Types of Flow of the Mixture. We determine the characteristic flow parameters of the phases that arise when the times of relaxation of the velocities and concentrations of the components change.

(1) Frozen flow occurs when $\tau_S, \tau_{m_2} \to \infty$ ($U_1 \neq U_2$ and $P_1 \neq P_2$). In this case, the speed of sound in the ith component a_i is known, we find the velocity behind the frozen shock wave $\tilde{U}_i = a_i^2/U_0$, and the velocities and pressures of the components are always different.

(2) Equilibrium flow occurs when $\tau_S, \tau_{m_2} \to 0$ ($U_1 = U_2$ and $P_1 = P_2$). It is characterized by the equilibrium speed of sound

$$C_e^2 = \frac{\xi_1}{m_1}\frac{m_1C - \rho\xi_1}{m_1^2C - \rho\xi_1},$$

and the velocities and pressures are equal. Here the velocities of the components in the final equilibrium state [1] behind the SW front can be determined analytically:

$$U_{\text{fin}} = \frac{2 - C + C_3 - \sqrt{(C - C_3)^2 + 4(C_3 - C_0^2C_{ef}^2)}}{2C_0}.$$

(3) Equilibrium-frozen flow occurs when $\tau_S \to 0$ and $\tau_{m_2} \neq 0, \infty$ ($U_1 = U_2$ and $P_1 \neq P_2$). The equilibrium-frozen speed of sound $C_{ef}^2 = \xi_1 + a^2\xi_2$ is obtained for this flow. The state behind the front of the equilibrium-frozen SW is defined as $\tilde{U} = C_{ef}^2/U_0$. The velocities of the components are equal, and the pressures are different.

(4) Frozen-equilibrium flow, for which $\tau_S \neq 0, \infty$ and $\tau_{m_2} \to 0$ ($U_1 \neq U_2$ and $P_1 = P_2$), is characterized by the frozen-equilibrium speed of sound

$$C_{fe}^2 = 1 + a^2\left(\frac{C_1}{C_2}\frac{\rho_2}{\rho_1}\right)^2.$$

The velocities of the components are different, and the pressures are equal.

It what follows, ordering of intermediate speeds of sound will be required. Our consideration showed that the following is valid.

Statement 1. *If* $m_{10} \in (0, m_*]$, *the chain of inequalities* $1 \leqslant C_e < C_{ef} < a < C_{fe}$ *is valid; if* $m_{10} \in (m_*, 1)$, *then* $C_e < 1 < C_{ef} < a < C_{fe}$, *where*

$$m_* = \frac{\bar{\rho}(a^2 - 1)}{C(1 - \bar{\rho})}.$$

3. Analysis of the Type of Steady Points of System (1.3). Classification of Shock-Wave Types. *Estimates of the Coefficients of the Secular Equation of the Jacobi Matrix.* To study the correctness of the formulation of problem (1.1), (1.2), we study the type of steady points of system (1.3). For this, we determine the eigenvalues of the Jacobi matrix of this system that satisfy the equation

$$\lambda^2 - \sigma\lambda + \Delta = 0. \tag{3.1}$$

Here

$$\sigma = -\frac{U^2 - C_{ef}^2}{U^2 - 1}\frac{Um_1}{\xi_1\tau_S(U^2 - a^2)} + \frac{\Omega U m_1 m_2}{\mu_2(U^2 - a^2)}\frac{U^2 - C_{fe}^2}{U^2 - 1};$$

$$\Delta = -\frac{\Omega m_1^2 m_2}{\xi_1\tau_S\mu_2(U^2 - a^2)}\frac{U^2 - C_e^2}{U^2 - 1}; \quad \Omega = -\left[\frac{\rho_1}{m_1^2} + \frac{\rho_2 a^2}{m_2^2}\right]; \quad U_1 = U_2 = U; \quad P_1 = P_2 = P.$$

We study the behavior of Δ as a function of (U, m_{10}). The sign of Δ is determined by the function $(U^2 - C_e^2)/[(U^2 - 1)(U^2 - a^2)]$. Thus, the qualitative behavior of $\Delta(U)$ for various values of m_{10} can be easily obtained from this formula. If $m_{10} \in (0, m_*)$, then $\Delta(U)$ is negative on the interval $U \in (0,1) \cup (C_e, a)$, and if $U \in (1, C_e) \cup (a, +\infty)$, it is positive. For $U = C_e$, Δ vanishes and has second-order discontinuities for $U = 1, a$. If $m_{10} = m_*$, there is only one discontinuity a, and the behavior of $\Delta(U)$ in the vicinity of this point is similar to the case described above. The function $\Delta(U)$ is negative for $U \in (0, a)$ and positive for $U \in (a, +\infty)$. If $m_{10} \in (m_*, 1)$, then $\Delta(U)$ is negative for $U \in (0, C_e) \cup (1, a)$ and positive for $U \in (C_e, 1) \cup (a, +\infty)$. When $U = C_e$, Δ vanishes. When $U = 1, a$, Δ has a second-order discontinuity. Finally, in all three cases, $\Delta(U)$ approaches zero asymptotically as $U \to +\infty$. We see that the sign of Δ is not determined by U.

If $\Delta < 0$, the discriminant $\mathcal{D} = \sigma^2 - 4\Delta$ is positive, and the values $\lambda_{1,2}$ are real. If $\Delta > 0$, an additional analysis is required. For this, we consider the discriminant $\mathcal{D}$ of Eq. (3.1), which determines the eigenvalues as a function of the ratio of the relaxation times $\chi = \tau_S/\tau_{m_2}$. Then, we have

$$\mathcal{D} = \sigma^2 - 4\Delta = \frac{1}{\tau_S^2} D\,[A\chi^2 + B\chi + C],$$

where

$$A = 4m_2^2\Omega^2(U^2 - C_{fe}^2)^2 > 0;$$

$$B = \frac{4\Omega m_2}{\xi_1}\left\{\frac{2}{U^2}(U^2 - 1)(U^2 - a^2)(U^2 - C_e^2) - (U^2 - C_{fe}^2)(U^2 - C_{ef}^2)\right\};$$

$$C = \frac{(U^2 - C_{ef}^2)^2}{\xi_1^2} > 0; \quad D = \frac{U^2 m_1^2}{(U^2 - 1)^2(U^2 - a^2)^2} > 0.$$

We seek the values of $\chi_\pm = (-B \pm \sqrt{B^2 - 4AC})/2C$ that determine the regions of definite sign of the function $\mathcal{D}(\chi)$. After some transformations for $\mathcal{D}_1(U) = B^2 - 4AC$, we can write

$$\mathcal{D}_1 = F(F - 1).$$

Here

$$F(U^2) = \frac{(U^2 - 1)(U^2 - a^2)(U^2 - C_e^2)}{U^2(U^2 - C_{ef}^2)(U^2 - C_{fe}^2)}.$$

Elementary estimates allow us to obtain

$$F = \begin{cases} < 1 & \text{for } U \in (1, C_e), \quad F(1) = F(C_e) = 0, \\ \leqslant 0 & \text{for } U \in [C_e, a), \\ \geqslant 0 & \text{for } U \in (C_{ef}, a), \quad F \in [0, \infty), \\ \leqslant 0 & \text{for } U \in [a, C_{fe}], \quad F \in [-\infty, 0), \\ > 1 & \text{for } U \in (C_{fe}, \infty]. \end{cases}$$

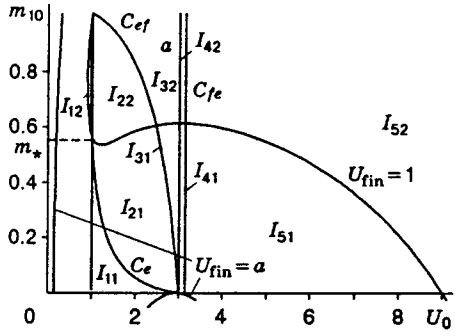

Fig. 1

We note that for $m_{10} \in (m_*, 1)$ the points 1 and C_e will change places in the pattern of the behavior of F described above. When $m_{10} = m_*$, the points 1 and C_e will merge. At the site of merging, the function F will have a maximum value on the interval $(0, C_{ef})$, which is equal to zero. As a result of this analysis we obtain

Statement 2. *If* $m_{10} \in (0, m_*)$, *we obtain the following estimates for* Δ *and* F:

(1) $U \in (1, C_e) = I_1$, $\Delta > 0$, *and* $0 < F < 1$;

(2) $U \in (C_e, C_{ef}) = I_2$, $\Delta < 0$, *and* $F < 0$;

(3) $U \in (C_{ef}, a) = I_3$, $\Delta < 0$, *and* $F > 0$ $[U \in (C_{ef}, C']$, $F \geqslant 1$ $U \in (C', a)$, *and* $F < 1]$;

(4) $U \in (a, C_{fe}) = I_4$, $\Delta > 0$, *and* $F < 0$;

(5) $U \in (C_{fe}, \infty) = I_5$, $\Delta > 0$, *and* $F > 1$.

If $m_{10} = m_*$, *the estimates for* Δ *and* F *are similar to those described above when* $m_{10} \in (0, m_*)$, *except for the region* I_1 *because* $C_e = 1$.

If $m_{10} \in (m_*, 1)$, *then for* Δ *and* F *we obtain estimates over regions that are similar to* (1)–(5), *in which the first two intervals are replaced by* $(C_e, 1)$ *and* $(1, C_{ef})$.

The eigenvalues and types of steady points of system (3.1).

(A) We consider the steady points in the initial state. We study the eigenvalues $\lambda_{1,2}$ of Eq. (3.1) using the previous statements for the corresponding regions (Fig. 1).

1. The region I_1 consists of the subregions I_{11} for $m_{10} \in (0, m_*)$ and I_{12} for $m_{10} \in (m_*, 1)$. For I_1, we have $\Delta > 0$ and $F \in (0, 1)$. Therefore, $\mathcal{D}_1 < 0$, and there are no roots $\chi_\pm$ of the equation $\mathcal{D}(\chi) = 0$. Hence, $\mathcal{D}(\chi) > 0$, and the singular point is a node.

2. In the region I_2, we have $\Delta < 0$ and $F < 0$. Hence, $\mathcal{D}_1 > 0$ and there are real roots of the equation

$$\chi_\pm = \frac{(U^2-1)(U^2-C_e^2)(U^2-a^2)}{\xi_1 m_2 U^2(-\Omega)(U^2-C_{fe}^2)^2}\left\{1-\frac{1}{2F} \pm \sqrt{1-\frac{1}{F}}\right\}.$$

The expression in braces is positive, and the sign of $\chi_\pm$ is determined by the sign of the relation $(U^2-1)(U^2-C_e^2)(U^2-a^2)$, which is negative everywhere in (C_e, a). Thus, $\chi_\pm < 0$ in I_2. Therefore, the inequality is valid, and we have a saddle point in this region.

3. The region I_3 is divided into two subregions: I_3', where $U \in (C_{ef}, C']$, and I_3'', where $U \in (C', a)$. There are real roots $\chi_\pm < 0$ in the region I_3'. Hence, we obtain a saddle point. In the region I_3'', we have $0 < F < 1$; therefore, $\chi_\pm$ are complex-conjugated, $\mathcal{D}(\chi) > 0$, $\Delta < 0$, and we obtain a saddle point.

4. In the region I_4, we have $F < 0$; hence, there are positive values of $\chi_\pm$. Thus, for $\chi \in (0, \chi_-) \cup (\chi_+, \infty)$ the discriminant $\mathcal{D}$ is positive. Furthermore, since $\Delta > 0$, the singular point is a node. For $\chi \in (\chi_-, \chi_+)$, we have $\mathcal{D} < 0$ and $\Delta > 0$, and the singular point is a focus.

5. In the region I_5, we have $F > 1$, and there are $\chi_\pm > 0$. Then the consideration reduces to the previous case with the only difference that a node is in the range $\chi \in (0, \chi_+) \cup (\chi_-, \infty)$, and a focus is on the interval $\chi \in (\chi_+, \chi_-)$.

The results lead to

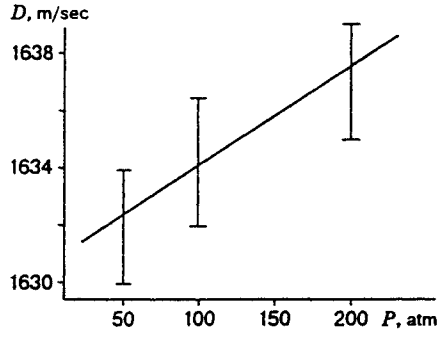

Fig. 2

Statement 3. *For $U_0 \in I_1$, the singular point is a node; for $U_0 \in (I_2, I_3)$, the singular point is a saddle; for $U_0 \in I_4$, the singular point is a node if $\chi \in (0, \chi_-) \cup (\chi_+, \infty)$ and a focus if $\chi \in (\chi_-, \chi_+)$; for $U_0 \in I_5$ the singular point is a node if $\chi \in (0, \chi_+) \cup (\chi_-, \infty)$ and a focus if $\chi \in (\chi_+, \chi_-)$.*

(B) We consider the steady points in the final state. By virtue of Cemplen's theory, $U_{\text{fin}} < C_{e,\text{fin}}$, and three variants are possible:

1. $0 < U_{\text{fin}} < 1 < C_{e,\text{fin}}$; then $\Delta < 0$ and the final point is a saddle.

2. $1 < U_{\text{fin}} < C_{e,\text{fin}}$; then $\Delta > 0$, $F \in (0,1)$, and $\mathcal{D}_1 < 0$. This means that there are no roots $\chi_\pm$ in the region of real numbers. Therefore, $\mathcal{D} > 0$ and the final point is a node.

3. $U_{\text{fin}} < C_{e,\text{fin}} < 1$; then, $\Delta < 0$, $\mathcal{D}(\chi) > 0$, and the final point is a saddle.

Thus, the following statement is valid.

Statement 4. *For $U_{\text{fin}} \in (0,1)$, the singular point is a saddle; for $U_{\text{fin}} \in (1, C_{e\text{fin}})$, the singular point is a node; for $U_{\text{fin}} \in (C_{e,\text{fin}}, 1)$, the singular point is a saddle.*

Summarizing the above considerations of the SW types (Fig. 1), we can formulate

Proposition. *If the boundary conditions for problem* (1.2) *and* (1.3) *at an infinitely distant point are such that:*

(1) *$U_0 \in (I_{21}, I_{31})$, then a solution $(U_1(\zeta), U_2(\zeta))$ exists in the class of continuously differentiable functions;*

(2) *$U_0 \in (I_{22}, I_{32})$, then a solution exists in the class of continuous functions for the second phase and in the class of discontinuous functions for the first component;*

(3) *$U_0 \in (I_{41}, I_{51})$, then a solution exists in the class of continuous functions for the light component and in the class of discontinuous functions for the heavy component;*

(4) *$U_0 \in (I_{42}, I_{52})$, then a solution exists in the class of discontinuous functions.*

Remark 1. Physically, flow (1) corresponds to fully dispersed shock waves in both phases, flow (2) to a dispersed SW in the heavy phase and a frozen SW in the light phase, flow (3) to a dispersed SW in the first component and a frozen SW in the second phase, and flow (4) corresponds to frozen SWs for both components of the mixture. The position of the frozen SW in the first phase is a free parameter of the problem.

Remark 2. In defining the region I_{kj} we do not include the vicinity of the line $U_{\text{fin}} = 1$, for which there is reason to believe that the solution in this region is transonic with internal singular points.

4. Discussion of Results of Numerical Calculations. We studied numerically the flow pattern of a mixture of water (the first phase) and silica sand (the second phase) in shock waves of various types. Figure 2 shows the velocity of the dispersed SW for $m_{10} = 0.4$ as a function of the equilibrium pressure behind the SW front (the solid line refers to the calculated results, and the vertical lines are the span of experimental data [7]). It can be seen that for moderate pressures in the mixture, the linear partial equations of state of the components allow one to describe the experimental data.

1. Let $U_0 \in (C_{e,0}, a)$ and $m_{10} \leqslant m^*$ (m^* is the value of m_{10} for which $U_{\text{fin}} = 1$). In this region of initial parameters, the SW is fully dispersed in both phases. As the volume concentration of water increases, we observe the distributions of parameters shown in Fig. 3, in which the flow in the SW is quasiequilibrium

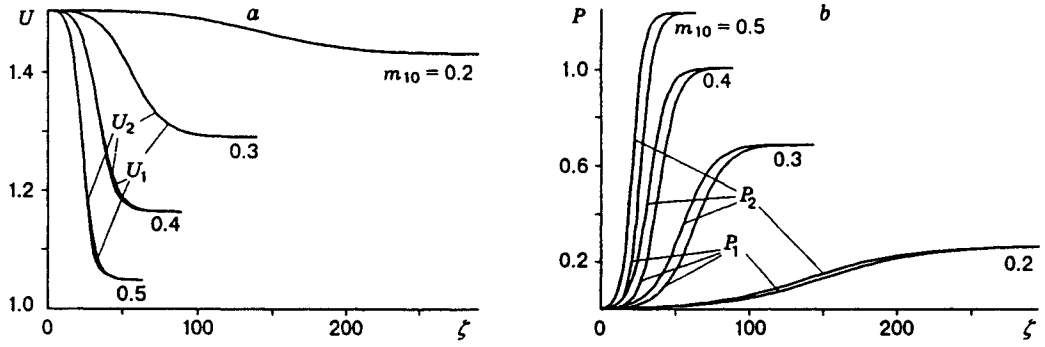

Fig. 3

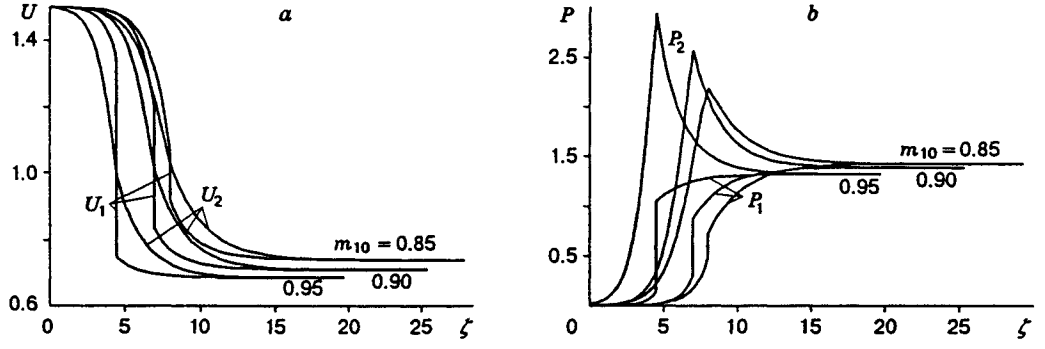

Fig. 4

in velocities. The SW width decreases as the liquid fraction increases, a more dramatic deceleration occurs, and, as a consequence, the increase in pressure is larger. In contrast to the velocity equilibrium, the phase pressures demonstrate nonequilibrium behavior. The difference in pressures is maximum at the SW center, and in the solid phase the pressure is larger than in the liquid phase.

A further increase in m_{10} changes the type of observed SW. The wave becomes a frozen-dispersed SW. We understand the frozen-dispersed SW as a flow that is adjacent asymptotically to the initial and final states at $\pm\infty$ and has a weak discontinuity in the second phase and a strong one in the first phase.

The mechanism of emergence of a frozen-dispersed SW is as follows. As m_{10} increases to m^*, the final velocity of the shock wave approaches the speed of sound in the first phase. For $m_{10} = m^*$, we have $U_{\text{fin}} = 1$. This motion of the mixture is marginal, and the singularity on the right-hand side of the first equation of (1.3) is evaluated. However, for $m_{10} > m^*$, we have $U_{\text{fin}} < 1$, and for attainment of an equilibrium state behind the SW front, transition through the speed of sound in the first phase is required. This is responsible for the appearance of a strong internal discontinuity in the liquid. In this case, the second phase has a weak discontinuity at this point of space. It can be seen (Fig. 4a and b) that as the liquid fraction of the mixture increases, the internal SW moves upstream and its intensity increases. The region of continuous flow ahead of the front of the internal SW decreases as m_{10} grows. It should be noted that continuous loading of the liquid occurs in the first phase. At the same time, loading is observed in the sand in the fore part of the frozen-dispersed SW (in the region located upstream of the internal SW), and unloading is observed in the rear part of the shock wave. The ratio of the maximum pressure of the second phase to the pressure of the liquid behind the front of the internal SW remains roughly equal to three when m_{10} changes. In addition, the pressure behind the SW front in the final equilibrium state exhibits nonmonotonous behavior with variation in the water content. There is a value of m_{10} after which an increase in m_{10} leads to a decrease in pressure behind the front. This is related to an increase in water content in the mixture.

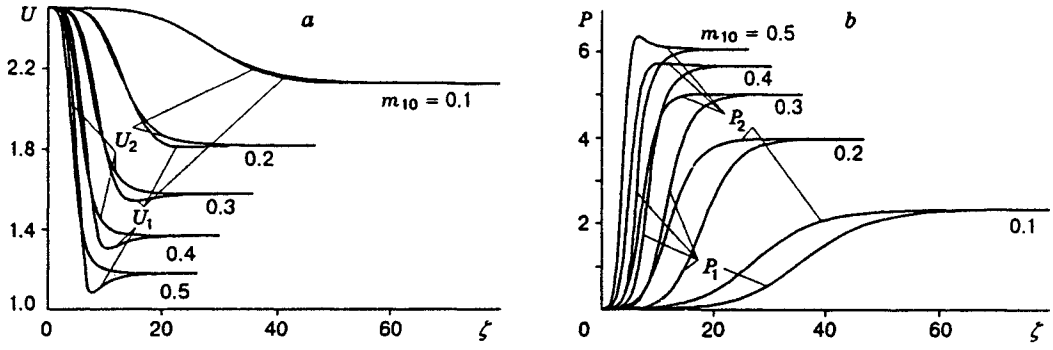

Fig. 5

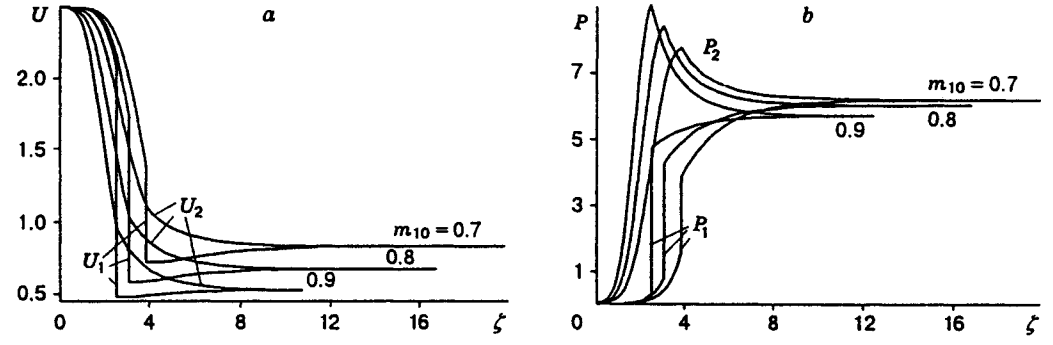

Fig. 6

2. We increase the SW velocity to $U_0 = 2.5$, remaining in the interval $(C_{e,0}, a)$ and $m_{10} < m^*$. The SW is a dispersed one, but the velocity of the liquid becomes nonmonotonous as m_{10} increases, as is shown in Fig. 5. In contrast to a SW with a small velocity ($U_0 = 1.5$), a flow in velocity quasiequilibrium is observed only for small m_{10} (see $m_{10} = 0.1$). The dispersed SW is divided into two regions. At the leading edge of the SW we have $U_1 > U_2$. At the rear edge of the SW behind the point $\zeta = \zeta_*$ $[U_1(\zeta_*) = U_2(\zeta_*)]$ we have $U_1 < U_2$, and the flow in this wave exhibits strong nonequilibrium in velocities. The velocity nonequilibrium is seen to increase as m_{10} increases. The flow with $m_{10} = 0.5$ contains a narrow zone in which dramatic deceleration of the phases occurs as if the flow undergoes a strong shock, behind which U_1 increases to its final value.

This nonmonotonous flow of the mixture exists until the minimum value of U_1 becomes equal to the speed of sound in the first phase. Since in this case equilibrium in velocities and pressures may not exist, a gradient catastrophe is possible, and there is no flow of this kind in a steady-state formulation.

The pressure in the light phase increases monotonically downstream (Fig. 5). The behavior of the pressure profile in the solid component depends on the initial volume concentration of the first phase. Figure 5 shows the transition from a monotonous pressure profile of the solid particles to a nonmonotonous profile. As m_{10} increases from 0.1 to 0.3, the pressure profile becomes flatter with approach to the final equilibrium state. For $m_{10} = 0.3$, the pressure in the solid particles reaches a certain "ledge" at the final stage. After that, a further increase in the initial volume concentration of the first phase gives rise to a pressure maximum in the second phase. The pressure maximum in the second phase is related to the increase in density of the solid particles due to their large mass.

As m_{10} increases, the flow of the dispersed SW becomes frozen-dispersed (Fig. 6). In contrast to case 1, however, the velocity of the first phase behind the front of the internal SW increases, while the particles are still decelerated. The mixture is in a strongly nonequilibrium state up to the internal shock. As the liquid is decelerated in the shock, the nonequilibrium of the phases decreases. The qualitative behavior of the pressure of the phases is similar to that described above for $U_0 = 1.5$.

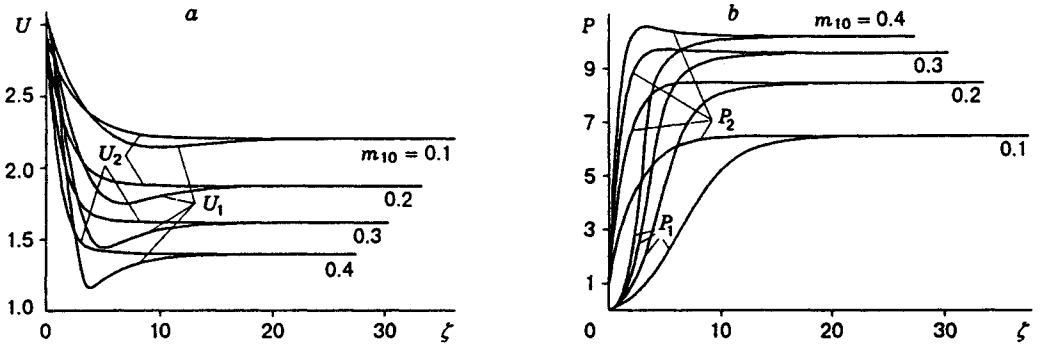

Fig. 7

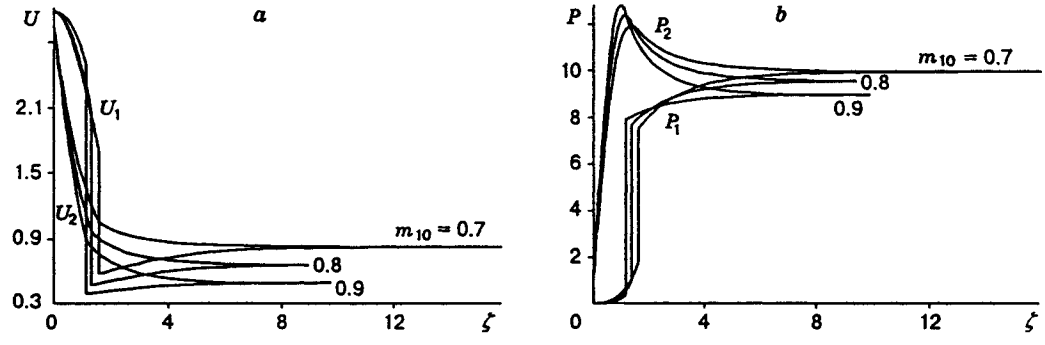

Fig. 8

3. Let $U_0 \in (a, C_{fe})$ and $U_0 = 3.05$ (Fig. 7). In this case, at small m_{10} the SW will be called a dispersed-frozen shock wave. There is a strong shock in the second component at the SW head [exit from the initial equilibrium state of a stable focus (a node) is accomplished by means of this shock]. Then the velocity of this component decreases monotonically until an equilibrium state is attained. The velocity of the light component changes continuously and demonstrates nonmonotonic behavior. In the flow the absolute value of $U_{1,\min}$ decreases and approaches unity as m_{10} increases. This type of flow requires special consideration.

The pressure in the first phase is monotonic, and the pressure in the second phase becomes nonmonotonic as m_{10} increases.

As m_{10} increases, the flow acquires a two-front configuration (Fig. 8), which is called a frozen SW. Here, at the SW head, there is a strong discontinuity in the second phase; the flow in the first phase is continuous. In the leading part of the frozen SW located upstream of the internal shock in the liquid, the flow is strongly nonequilibrium. The degree of nonequilibrium decreases after deceleration of the liquid in the internal shock. The particles are still decelerated, whereas the liquid, to which momentum is transferred from the particles, is accelerated until the phase velocities become equal.

4. Increasing the velocity U_0 to values within the interval (C_{fe}, a^2), we obtain the following flow patterns. For $U_0 = 3.3$, the velocities and pressures behave qualitatively similarly to the case $U_0 = 3.05$. The difference lies in the SW intensity, which increases with increase in U_0.

5. Remarks on the calculational technique. The calculation of fully dispersed shock waves reduced to determining the trajectory passing from the saddle to the node and involved no difficulties.

To determine flows with an internal SW (motion of the mixture of the type of a frozen-dispersed SW) we used the following calculation algorithm. An exit from the initial and final steady points (saddles) was performed analytically along the separatrix in the unstable direction. Having calculated the appropriate separatrices, we connected them through the SW conditions in the first phase. The position of the internal SW was the parameter to be found.

The dispersed-frozen SW was calculated as follows. An exit from the initial state was performed by introducing a SW in the second phase and subsequent calculation of the trajectory up to attainment of the final equilibrium state (node).

To determine the flow parameters with frozen shock waves for both components, we used the following algorithm: an exit from the initial state was performed by introducing a SW in the second phase; the trajectory passing to the final equilibrium state was found by choosing the SW position in the light component using the technique described above for the frozen-dispersed SW.

5. Conclusions. The structure of shock waves in the form of dispersed and frozen shock waves with one- and two-front configurations is described on the basis of a mathematical model for the flow of a mixture of two condensed components with different velocities and pressures.

It is shown that this model adequately describes the experimental data obtained by G. M. Lyakhov for the dependence of the dispersed-SW velocity on the equilibrium pressure behind its front.

A chart of possible types of motion of the mixture is constructed in a plane with coordinates m_{10} and U_0. The calculated data illustrating these types of flow are presented and analyzed.

REFERENCES

1. A. V. Fedorov, "Mathematical description of the flow of a mixture of condensed materials at high pressures," in: *Physical Gas Dynamics of Reactive Media* [in Russian], Nauka, Novosibirsk (1990), pp. 119–128.
2. A. V. Fedorov, "Shock-wave structure in a mixture of two solids (a hydrodynamic approximation)," *Model. Mekh.*, **5(22)**, No. 4, 135–158 (1991).
3. A. V. Fedorov, "Shock-wave structure in a heterogeneous mixture of two solids with equal pressures of the components," in: *Numerical Methods of Solving Problems of Elasticity and Plasticity* (Collection of scientific papers) [in Russian], Inst. of Theor. and Appl. Mechanics, Novosibirsk (1992), pp. 235–249.
4. A. V. Fedorov and N. N. Fedorova, "The structure, propagation, and reflection of shock waves in a mixture of two solids (a hydrodynamic approximation)," *Prikl. Mekh. Tekh. Fiz.*, No. 4, 10–18 (1992).
5. E. V. Varlamov and A. V. Fedorov, "A traveling wave in a nonisothermal mixture of two solids," *Model. Mekh.*, **5(22)**, No. 3, 14–26 (1991).
6. M. R. Baer and J. W. Nunziato, "A two-phase mixture theory for the deflagration-to-detonation transition (DDT) in reactive granular materials," *J. Multiphase Flow*, **12**, No. 6, 861–889 (1986).
7. G. M. Lyakhov, *Fundamentals of Explosion Dynamics in Ground and Liquid Media* [in Russian], Nedra, Moscow (1964).